



Effects of a flexible joint on instability of a free-free jointed bipartite beam under the follower and transversal forces

Saied IRANI[†], Omid KAVIANIPOUR

(Department of Aerospace Engineering, K. N. Toosi University of Technology, Tehran, Iran)

[†]E-mail: irani@kntu.ac.ir

Received Aug. 7, 2008; Revision accepted Feb. 9, 2009; Crosschecked July 22, 2009

Abstract: This paper deals with the problem of the instability regions of a free-free flexible jointed bipartite beam under the follower and transversal forces as a realistic simulation of a two-stage aerospace structure. The aim of this study is to analyze the effects of the characteristics of a flexible joint on the beam instability to use maximum bearable propulsion force. A parametric study is conducted to investigate the effects of the stiffness and the location of the joint on the critical follower force by the Ritz method and the Newmark method, then to research the vibrational properties of the structure. It has been shown that the nature of instability is quite unpredictable and dependent on the stiffness and the location of the joint. The increase of the follower force or the transversal force will increase the vibration of the model and consequently cause a destructive phenomenon in the control system of the aerospace structure. Furthermore, this paper introduces a new concept of the parametric approach to analyze the characteristics effects of a flexible two-stage aerospace structure joint design.

Key words: Two stage to orbit launch vehicle (TSTO LV), Beam instability, Follower force, Ritz's method, Newmark's method
doi:10.1631/jzus.A0820621 **Document code:** A **CLC number:** O34

INTRODUCTION

The stability of the beams under the axial or follower force, which can be applied to many aerospace structures, is of vital importance and is in the interest of many researchers. In fact the axial or follower force represents a model for the propulsion force (thrust). The direction of the axial force is assumed to be immovable while the direction of the follower force is always perpendicular to the cross surface of the beam and changes with the beam deflections. The critical axial force normally causes the static instability (divergence) and the follower force may cause static or dynamic instability (flutter). Divergence happens when the vibration frequency of the system becomes zero and flutter occurs when two natural frequencies of the systems converge together. The very first researchers in this field used a simple structural dynamics model of the beam and did not consider the instability effects of the axial or the follower forces where these forces change the structural

behavior of the beam significantly. So some researchers studied the instability effects of the axial force while some others studied the follower force. Many researchers have focused on analyzing the problem of the single stage to orbit launch vehicles (SSTO LVs). In addition to the SSTO LVs, two stage to orbit launch vehicle (TSTO LV) is also an important topic in the aerospace engineering fields.

In this paper, the TSTO LV model for an aerospace structure is studied and the instability of this structure is analyzed. The structure is modeled by a jointed bipartite beam (stages 1 and 2) under the follower and transversal forces, which is an acceptable model for such structures with the propulsion force and the controller force (the actuators force to control and guide the TSTO LV). And the separation and adapter interface equipments between stage 1 and stage 2 are modeled by two shear and rotational springs (Fig.1). The aim of this study is to analyze the instability of TSTO LVs considering the propulsion and the controller forces so the aerospace structure

could run on its maximum bearable propulsion force. The effects of the length of each stage and the stiffness of the springs on the vibrational instability of the structure are investigated. This study presents an approximation method as a design tool to find the optimized length of each stage and the stiffness for the springs. This parametric study also introduces a new concept to analyze the instability effects of the characteristics of a flexible joint of a two-stage aerospace structure that could be considered during its design.

It will also be shown that increasing the follower or transversal forces results in an increase in the vibrational movement of the model. This in turn causes an inaccuracy in the control and guidance systems and performance degradation in the actuators. The Ritz method is used in the calculations of the system frequencies and the Newmark method is employed for the study of the vibrational properties of the model.

Bokaian (1988) obtained an analytical characteristic equation for uniform beams under constant compressive axial load and considered some approximate relations for the buckling load and variation of normalized natural frequency with normalized axial force. Thana and Ameen (2007) addressed the dynamic stability problem of columns and frames subjected to axially applied periodic loads. The finite element method (FEM) was used in their work to analyze dynamic stability problems of columns. Hassanpour *et al.* (2007) analyzed the exact solution of free vibration of a beam with a concentrated mass within its intervals when the beam was subjected to axial loadings. They determined the exact mode shapes of vibration, which were necessary in the study of the time-domain response of sensors and determination of stability regions. Joshi (1995) established a simple method to determine the mode shapes and the natural frequencies of a non-uniform beam subjected to rear end propulsion force. Another research to obtain the governing vibration equations and the stability of a beam under axial force was carried out by Nihous (1997). Pourtakdoust and Assadian (2004) modeled a free-free Bernoulli beam under an axial force. The 3D elastic equations of vibration were solved by the FEM. Only the divergence was found and shown in their work. And finally the elastic equations beside the equations of motion were simulated in a controller loop by the authors in their last work. It was shown that the oscillations of the actuators were increased when the

axial force was applied. Langthjem and Sugiyama (1999) studied a cantilever beam under a follower force with a tip mass to optimize the design of the beam. Another research in instability of a non-uniform cantilever beam under a follower force was done using the FEM (Au *et al.*, 1999).

Young and Juan (2003) presented a study of non-linear response of a fluttered, cantilevered beam subjected to a random follower force at the free end. Wang (2004) investigated a comprehensive analysis of the stability of a cracked beam subjected to a follower compressive load. Luongo and Di Egidio (2006) studied an internally constrained planar beam, equipped with a lumped visco-elastic device and loaded by a follower force. Paolone *et al.* (2006) analyzed the stability of a cantilever elastic beam with rectangular cross-section under the action of a follower tangential force and a bending conservative couple at the free end. Elfelsoufi and Azrar (2006) presented a mathematical model based on integral equations for numerical investigations of stability analyses of damped beams subjected to sub-tangential follower forces.

Many researches were also published for the cantilever beam under a follower force with damping (Detinko, 2003; Ryu and Sugiyama, 2003; Di Egidio *et al.*, 2007; Lee *et al.*, 2007). Sugiyama and Langthjem (2007) studied a cantilever beam under a follower force with proportional damping. Both internal (material) and external (viscous fluid) damping were considered. Tomsaki *et al.* (2007) presented the results of theoretical and numerical studies on the slender, geometrically nonlinear system supported at the loaded end by a spring of a linear characteristic and subjected to non-conservative (generalized Beck's) loading.

The large-deflection problem of a non-uniform spring-hinged cantilever beam under a tip-concentrated follower force was considered by Shvartsman (2007). Shape optimization was used to optimize the critical load of an Euler-Bernoulli cantilever beam with constant volume subjected to a tangential compressive tip load and/or a tangential compressive load arbitrarily distributed along the beam by Katsikadelis and Tsiatas (2007). de Rosa *et al.* (2008) dealt with the dynamic behaviour of a clamped beam subjected to a sub-tangential follower force at the free end. Djondjorov and Vassilev (2008) studied the dynamic stability of a cantilevered Timoshenko beam

lying on an elastic foundation of Winkler type and subjected to a tangential follower force.

Attard *et al.* (2008) investigated the dynamic stability behaviors of damped Beck's columns subjected to sub-tangential follower forces using the fifth-order Hermitian beam elements. Marzani *et al.* (2008) applied the generalized differential quadrature (GDQ) method to solve classical and non-classical non-conservative stability problems. The governing differential equation for a nonuniform column subjected to an arbitrary distribution of compressive subtangential follower forces was obtained. Beal (1965) investigated a uniform free-free beam under an end follower force. He introduced a direction control mechanism for the follower force to eliminate the tumbling instability of a free-free beam under a follower force. He also showed that, in the absence of the control system, the critical follower force magnitude is associated with coalescence of the two lowest bending frequencies. When the control system was included, it was found that the critical follower force magnitude only corresponded to a reduction of the lowest frequency of zero. Wu (1975) studied the stability of a free-free beam under a controlled follower force using finite element discretization with an adjoint formulation.

Park and Mote (1985) studied the maximum controlled follower force on a free-free beam carrying a concentrated mass. They predicted the location and the magnitude of the additional concentrated mass, and the location and the gain of the follower force direction control sensor that permit the follower force to be maximized for stable transverse motion of the beam. Park (1987) investigated a uniform free-free Timoshenko beam under an end follower force with controlled direction. A finite element model of the beam transverse motion in the plane was formulated through the extended Hamilton's principle. The analysis showed that the effects of the rotary inertia and shear deformation parameters on the stable transverse motion of the beam are significant in certain ranges. Sato (1991) developed the governing equation of motion of a Timoshenko beam under a follower force using the Hamilton's principle.

Mladenov and Sugiyama (1997) dealt with the stability of a flexible space structure subjected to an end follower force. The model consisted of two viscoelastic beams interconnected by two kinds of joints. One of the joints was composed of a rotational vis-

coelastic spring while the other was a shear viscoelastic spring. Bending flutter or post-flutter divergence showed a dependence on the joint rigidity and the internal damping. Kim and Choo (1998) analyzed the dynamic stability of a free-free Timoshenko beam with a concentrated mass subjected to a pulsating follower force. They studied the instability effects of axial location and translation inertia of the concentrated mass, and also examined the change of combination resonance types, the relationship between critical forces and widths of instability regions considering the shear deformation.

MATHEMATICAL MODELING

Fig.1 shows the assumed model for the beam where two springs represent the joint of the two parts of the beam. The propulsion force is modeled by a follower force and the controller force is shown as the transversal force. In Fig.1, x_s and x_{F_0} are the sensors (inertial measuring units) location and the controller force location, respectively. The beam is a Bernoulli beam and has been assumed to be axially rigid. The gravity force is ignored.

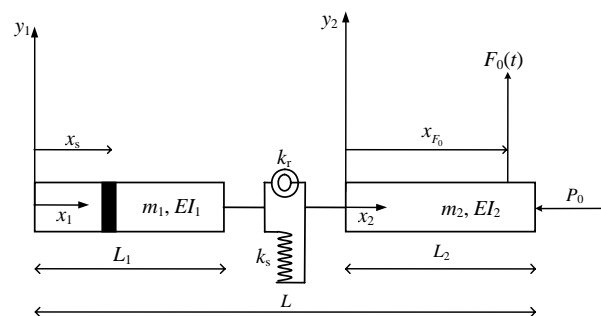


Fig.1 The simple model of a two stage to orbit launch vehicle as a jointed bipartite beam

L_1 , m_1 , EI_1 are the length, mass per unit length, and bending stiffness of the first part of the beam (stage 1), respectively. L_2 , m_2 , EI_2 are the length, mass per unit length, and bending stiffness of the second part (stage 2), respectively. k_r and k_s are the stiffness of the rotational and shear springs, respectively. x_1 - y_1 and x_2 - y_2 are two independent coordinates of two parts of the beam. P_0 is the follower force and $F_0(t)$ is the transversal force applied at x_{F_0} .

Energy method

One of the most effective methods to derive the governing equations is the Energy Method. Having all of the energies in the system and applying the Hamilton Principle, the governing equations could be derived accurately. The Hamilton Principle is

(Meirovitch, 1997)

$$\delta \int_{t_1}^{t_2} (T - V + W_c) dt + \int_{t_1}^{t_2} \delta W_{nc} dt = 0, \quad (1)$$

where δ is the variation, t is time, T is the kinetic energy, V is the potential energy, W_c is the work done by conservative forces, and W_{nc} is the work done by non-conservative forces. For the presented model in Fig.1, the above items could be presented as

$$\begin{aligned} T &= \frac{1}{2} \int_0^{L_1} m_1 \left(\frac{\partial y_1}{\partial t} \right)^2 dx_1 + \frac{1}{2} \int_0^{L_2} m_2 \left(\frac{\partial y_2}{\partial t} \right)^2 dx_2, \\ V &= \frac{1}{2} \int_0^{L_1} EI_1 \left(\frac{\partial^2 y_1}{\partial x_1^2} \right)^2 dx_1 + \frac{1}{2} \int_0^{L_2} EI_2 \left(\frac{\partial^2 y_2}{\partial x_2^2} \right)^2 dx_2 \\ &\quad + \frac{1}{2} k_r \left(\frac{\partial y_1}{\partial x_1} \bigg|_{x_1=L_1} - \frac{\partial y_2}{\partial x_2} \bigg|_{x_2=0} \right)^2 + \frac{1}{2} k_s \left(y_1|_{x_1=L_1} - y_2|_{x_2=0} \right)^2, \quad (2) \\ W_c &= \frac{1}{2} \int_0^{L_1} P_1 \left(\frac{\partial y_1}{\partial x_1} \right)^2 dx_1 + \frac{1}{2} \int_0^{L_2} P_2 \left(\frac{\partial y_2}{\partial x_2} \right)^2 dx_2, \\ \delta W_{nc1} &= -P_0 \left(\frac{\partial y_2}{\partial x_2} \bigg|_{x_2=L_2} \right) \delta y_2|_{x_2=L_2}, \\ \delta W_{nc2} &= F_0(t) \delta y_2|_{x_2=x_{F_0}}, \end{aligned}$$

where L_1 , m_1 , EI_1 , and P_1 are the length, mass per unit length, bending stiffness, and axial force of the first part of the beam respectively, and L_2 , m_2 , EI_2 , and P_2 are the length, mass per unit length, bending stiffness, and axial force of the second part respectively. k_r and k_s are the stiffnesses of the rotational and shear springs, respectively. P_0 is the follower force and $F_0(t)$ is the transversal force applied at x_{F_0} .

To calculate the axial force along each part of the beam, the dynamics equilibrium can be used (Wu, 1975):

$$\begin{cases} P_1 = \frac{x_1}{L_1 + L_2} P_0, & 0 \leq x_1 \leq L_1, \\ P_2 = \frac{L_1 + x_2}{L_1 + L_2} P_0, & 0 \leq x_2 \leq L_2. \end{cases} \quad (3)$$

As the effects of the bending stiffness are not in the interest of this study and mostly the effects of stiffness and the joint location are considered, it has been assumed that the two parts of the beam are uni-

form and have similar characteristics, and

$$m_1 = m_2 = m, \quad EI_1 = EI_2 = EI. \quad (4)$$

The dimension of the joint is assumed to be small and is neglected, so

$$L_1 + L_2 = L. \quad (5)$$

To simplify Eq.(5), non-dimensional parameters are introduced as follows:

$$\begin{aligned} \bar{x}_1 &= \frac{x_1}{L}, \quad \bar{x}_2 = \frac{x_2}{L}, \quad \bar{y}_1 = \frac{y_1}{L}, \quad \bar{y}_2 = \frac{y_2}{L}, \quad \bar{L}_1 = \frac{L_1}{L}, \\ \bar{t} &= t \left(\frac{EI}{mL^4} \right)^{0.5}, \quad \bar{k}_r = \frac{k_r L}{EI}, \quad \bar{k}_s = \frac{k_s L^3}{EI}, \\ \bar{P}_0 &= \frac{P_0 L^2}{EI}, \quad \bar{F}_0 = \frac{F_0 L^2}{EI}. \end{aligned} \quad (6)$$

As the governing differential equation cannot be solved analytically, an approximation method must be used. Utilizing the Ritz method via using Hamilton's principle following Hodges and Pierce (2002), a simplified matrix form equation can be derived when the response is approximated by the following series:

$$\begin{cases} \bar{y}_1(\bar{x}_1, \bar{t}) = \sum_{i=1}^N \phi_{1i}(\bar{x}_1) q_i(\bar{t}), \\ \bar{y}_2(\bar{x}_2, \bar{t}) = \sum_{i=1}^N \phi_{2i}(\bar{x}_2) q_i(\bar{t}), \end{cases} \quad (7)$$

where $\phi_{1i}(\bar{x}_1)$ and $\phi_{2i}(\bar{x}_1)$ are admissible functions for stages 1 and 2 of the beam respectively, and $q_i(t)$ is a generalized coordinate. The following simplified matrix form can be derived:

$$\mathbf{M} \ddot{\mathbf{q}} + \mathbf{K} \mathbf{q} = \mathbf{Q}, \quad (8)$$

where $\ddot{\mathbf{q}} = \frac{d^2 \mathbf{q}}{dt^2}$, \mathbf{M} is the mass matrix, \mathbf{K} is the stiffness matrix and \mathbf{Q} is the generalized force vector and can be described as

$$M_{ij} = \int_0^{\bar{L}_1} \phi_{1i} \phi_{1j} d\bar{x}_1 + \int_0^{1-\bar{L}_1} \phi_{2i} \phi_{2j} d\bar{x}_2,$$

$$\begin{aligned}
K_{ij} = & \int_0^{\bar{L}_1} \phi_{1i}'' \phi_{1j}'' d\bar{x}_1 + \int_0^{1-\bar{L}_1} \phi_{2i}'' \phi_{2j}'' d\bar{x}_2 \\
& + \bar{k}_r [\phi_{1i}'(\bar{L}_1) - \phi_{2i}'(0)] [\phi_{1j}'(\bar{L}_1) - \phi_{2j}'(0)] \\
& + \bar{k}_s [\phi_{1i}(\bar{L}_1) - \phi_{2i}(0)] [\phi_{1j}(\bar{L}_1) - \phi_{2j}(0)] \\
& - \bar{P}_0 \left[\int_0^{\bar{L}_1} \bar{x}_1 \phi_{1i}' \phi_{1j}' d\bar{x}_1 + \int_0^{1-\bar{L}_1} (\bar{L}_1 + \bar{x}_2) \phi_{2i}' \phi_{2j}' d\bar{x}_2 \right] \quad (9) \\
& + \bar{P}_0 \phi_{2i}'(1 - \bar{L}_1) \phi_{2j}'(1 - \bar{L}_1), \\
Q_j = & \bar{F}_0(\bar{t}) \phi_{2j}(\bar{x}_{F_0}), \\
i, j = & 1, 2, \dots, N,
\end{aligned}$$

where $\varphi' = \frac{d\varphi}{d\bar{x}}$ and $\varphi'' = \frac{d^2\varphi}{d\bar{x}^2}$.

In Eq.(9), the partial differential equation is converted to a set of ordinary differential equations using the approximation method.

ADMISSIBLE FUNCTIONS

In general the admissible functions $\varphi_i(x)$ should satisfy four conditions: (1) At least must satisfy all geometric boundary conditions; (2) Must be continuous and differentiable to the highest spatial derivative; (3) Should be a complete function; (4) Must be linearly independent.

The mode shapes of a free-free jointed bipartite beam satisfy the above conditions and have been used in this study. As the first two rigid body modes are not involved in instability, they are not considered as the admissible functions (Beal, 1965).

$$\phi_i(\bar{x}) = \begin{cases} \phi_1(\bar{x}_1) = A_1 \sin(\lambda_i \bar{x}_1) + A_2 \cos(\lambda_i \bar{x}_1) \\ \quad + A_3 \sinh(\lambda_i \bar{x}_1) + A_4 \cosh(\lambda_i \bar{x}_1), \\ \quad 0 \leq \bar{x}_1 \leq \bar{L}_1, \\ \phi_2(\bar{x}_2) = A_5 \sin(\lambda_i \bar{x}_2) + A_6 \cos(\lambda_i \bar{x}_2) \\ \quad + A_7 \sinh(\lambda_i \bar{x}_2) + A_8 \cosh(\lambda_i \bar{x}_2), \\ \quad 0 \leq \bar{x}_2 \leq 1 - \bar{L}_1, \end{cases} \quad (10)$$

where A_1, A_2, \dots, A_8 are mode shape coefficients, and

$$\lambda^4 = \frac{mL^4}{EI} \omega_i^2, \quad (11)$$

where ω_i is the natural frequency of the free-free jointed bipartite beam.

The natural boundary conditions in the assumed model are

$$\begin{cases} \phi_1''(0) = 0, \quad \phi_1'''(0) = 0, \\ \phi_2''(1 - \bar{L}_1) = 0, \quad \phi_2'''(1 - \bar{L}_1) = 0, \\ \phi_1''(\bar{L}_1) = \phi_2''(0) = \bar{k}_r [\phi_1'(\bar{L}_1) - \phi_2'(0)], \\ \phi_1'''(\bar{L}_1) = \phi_2'''(0) = \bar{k}_s [\phi_1(\bar{L}_1) - \phi_2(0)], \end{cases} \quad (12)$$

where $\varphi''' = \frac{d^3\varphi}{d\bar{x}^3}$.

The first four mode shapes of the free-free jointed bipartite beam for \bar{L}_1 and $\bar{k}_r = \bar{k}_s = 3000$ are shown in Fig.2. Incontinuity of the mode shapes is clear in the higher frequencies because \bar{k}_r and \bar{k}_s are high.

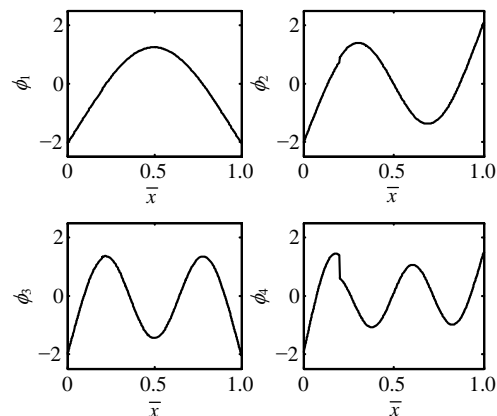


Fig.2 The first four mode shapes of the free-free jointed bipartite beam for $\bar{L}_1=0.2$ and $\bar{k}_r = \bar{k}_s = 3000$

RESULTS AND DISCUSSION

In this research, the effects of the location of the joint on the critical follower force \bar{P}_{ocr} were analyzed by choosing four different locations, i.e., $\bar{L}_1=0.2, 0.4, 0.6, 0.8$. Also the instability effects of the stiffness of the spring joints are investigated by changing \bar{k}_r from 1×10^0 to 1×10^4 and \bar{k}_s from 1×10^2 to 1×10^4 . One of the aims of this work is to find the first or the lowest critical follower force \bar{P}_0 causing the instability in the system.

The critical follower force is very dependent on the joint location and the springs' stiffness. These

parameters also affect the type and characteristics of the instability from divergence to flutter or vice versa. In the flutter regime, the joint location and the springs stiffness also change the cause of the flutter from merging the first and the second natural frequencies to merging the second and the third ones, or the third and the fourth ones. It is worth mentioning that only the first four natural frequencies were investigated in this study. And the number of mode shapes used for the Ritz method is 8 ($N=8$).

To obtain the variation of the natural frequencies by the follower force, one needs to set the right term of Eq.(8) to zero (in other words, sets $\bar{F}_0(\bar{r}) = 0$) and to assume that the homogeneous response is in the form of

$$\mathbf{q}_j = \bar{\mathbf{q}}_j e^{i\bar{\lambda}\bar{r}}, \quad i = \sqrt{-1}, \quad \bar{\lambda} = \lambda / \lambda_1, \quad (13)$$

where $\bar{\mathbf{q}}_j$ is a constant vector, and λ_1 is the first natural frequency for $\bar{P}_0 = 0$. So, $\bar{\lambda}$ is the non-dimensional frequency of the system with non-zero of \bar{P}_0 .

Case $\bar{L}_1 = 0.2$

For the case $\bar{L}_1 = 0.2$, the joint is located at one fifth of the beam from the top. The results for this case show that for all of the values of \bar{k}_r and \bar{k}_s , the dominant instability is flutter and is due to the convergence of the first and the second natural frequencies. Fig.3 shows the variations of the first and second non-dimensional natural frequencies versus the non-dimensional follower force \bar{P}_0 for particular values of \bar{k}_r and \bar{k}_s . In Fig.4 the effects of variation of \bar{k}_r and \bar{k}_s on the non-dimensional critical follower force are presented.

Case $\bar{L}_1 = 0.4$

When $\bar{L}_1 = 0.4$, the joint is located at two fifths of the beam from the top. The results for this case show that for all values of \bar{k}_r and \bar{k}_s , still the dominant instability is flutter and is mostly due to the convergence of the first and the second natural frequencies. Only when \bar{k}_r is low and \bar{k}_s is high, the

second and the third natural frequencies converge and flutter happens. Fig.5 shows the variations of the first, the second and the third non-dimensional natural frequencies versus the non-dimensional follower force \bar{P}_0 for particular values of \bar{k}_r and \bar{k}_s . In Fig.6 the effects of variation of \bar{k}_r and \bar{k}_s on the non-dimensional critical follower force (\bar{P}_{0cr}) are presented.

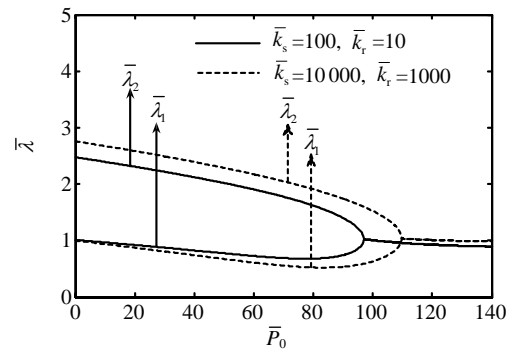


Fig.3 Variations of the first and second non-dimensional natural frequencies vs the non-dimensional follower force \bar{P}_0 for particular values of \bar{k}_r and \bar{k}_s when $\bar{L}_1=0.2$

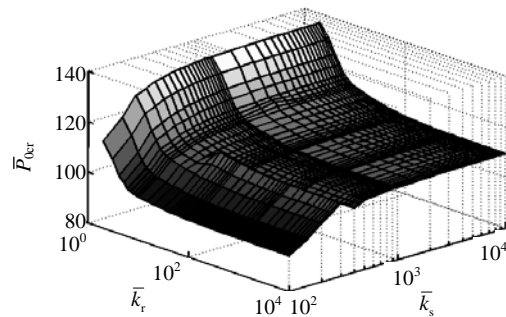


Fig.4 Effects of variation of \bar{k}_r and \bar{k}_s on the non-dimensional critical follower force (\bar{P}_{0cr}) when $\bar{L}_1=0.2$

Case $\bar{L}_1 = 0.6$

The results for this case show some interesting results. When the joint location gets closer to the end (where the follower force is applied), the instability occurs due to divergence (the first natural frequency becomes zero) or flutter (due to the convergence of the first and the second natural frequencies) depending on the springs stiffness. For small \bar{k}_r the first natural frequency decreases when the follower force is increased and becomes zero (divergence). But

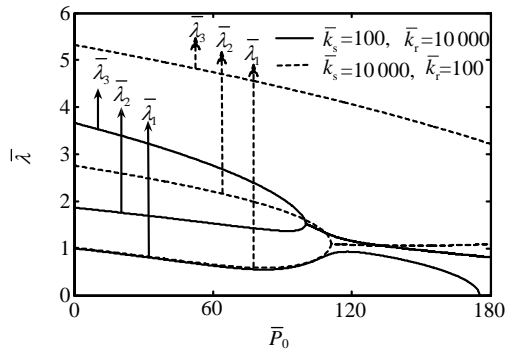


Fig.5 Variations of the first, the second and the third non-dimensional natural frequencies vs the non-dimensional follower force \bar{P}_0 for particular values of \bar{k}_r and \bar{k}_s when $\bar{L}_1=0.4$

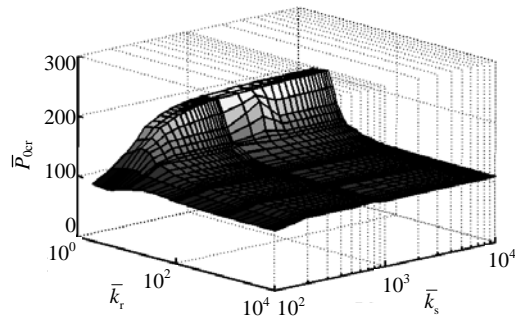


Fig.6 Effects of variation of \bar{k}_r and \bar{k}_s on the non-dimensional critical follower force (\bar{P}_{0cr}) when $\bar{L}_1=0.4$

when \bar{k}_r is higher, the dominant mode of instability becomes flutter.

Fig.7 shows the variations of the first and the second non-dimensional natural frequencies versus the non-dimensional follower force \bar{P}_0 for particular values of \bar{k}_r and \bar{k}_s . In Fig.8 the effects of variation of \bar{k}_r and \bar{k}_s on the non-dimensional critical follower force (\bar{P}_{0cr}) are presented.

The sharp risen section of Fig.8 is the border between divergence instability (small values of \bar{k}_r) and the flutter instability (high values of \bar{k}_r). For a constant value of \bar{k}_s , the critical follower force in divergence in this case is less than the one in flutter. Also, when the flutter is the dominant instability mode, \bar{k}_r will increase, and the critical follower force will decrease. It means that instability happens with lower values of the follower force.

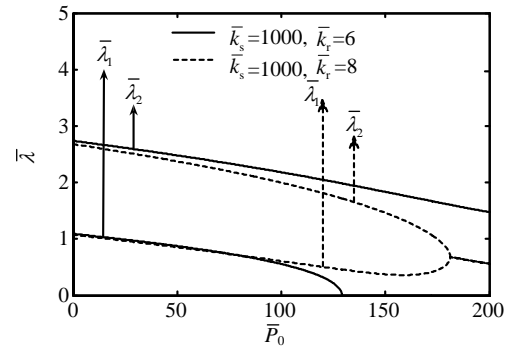


Fig.7 Variations of the first and the second non-dimensional natural frequencies vs the non-dimensional follower force \bar{P}_0 for particular values of \bar{k}_r and \bar{k}_s when $\bar{L}_1=0.6$

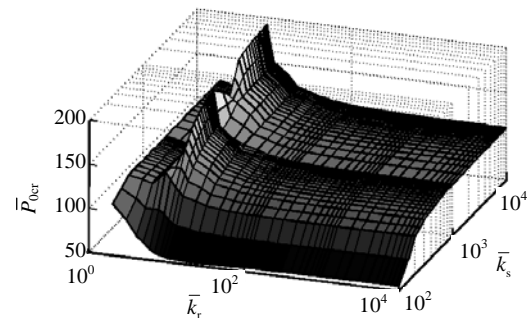


Fig.8 Effects of variation of \bar{k}_r and \bar{k}_s on the non-dimensional critical follower force (\bar{P}_{0cr}) when $\bar{L}_1=0.6$

Case $\bar{L}_1 = 0.8$

The results for this case show that when the joint location gets near to the end (where the follower force is applied), the instability occurs unpredictably due to divergence (the first natural frequency becomes zero) or flutter (due to the convergence of the first and the second or the third and the fourth natural frequencies) depending on the springs stiffness. In Figs.9 and 10, the variation of the first and the second non-dimensional natural frequencies versus the non-dimensional follower force \bar{P}_0 for two sets of \bar{k}_r and \bar{k}_s are shown. In Fig.11, the effects of variation of \bar{k}_r and \bar{k}_s on the non-dimensional critical follower force (\bar{P}_{0cr}) are presented. The main reason for the plunge in the surface is that for some values of \bar{k}_r and \bar{k}_s , the first instability occurs when the third and the fourth natural frequencies are converged. For example, when $\bar{k}_r=200$ and $\bar{k}_s=600$, the convergence of

the third and the fourth natural frequencies is the first instability as shown in Fig.12.

To verify the current results, when the joint of the bipartite beam is in high stiffness, it should represent approximately a uniform beam and the critical follower force in both models should be close to each other. This fact could be clearly found in Figs.4, 6, 8 and 11. When \bar{k}_r and \bar{k}_s are increasing, the value of critical follower force of this model is close to that of the uniform beam ($\bar{P}_{ocr}=109.9$, Beal, 1965).

DISPLACEMENT ANALYSIS

This research is to analyze the displacement of a point in the beam near the tip where normally the IMUs are located. The analysis of displacements and vibrations of this point over time is crucial for any control system used in the aerospace structure.

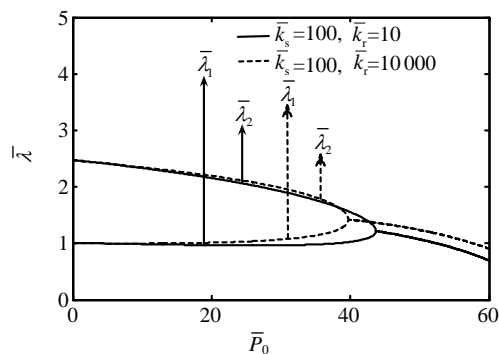


Fig.9 Variations of the first and second non-dimensional natural frequencies vs the non-dimensional follower force \bar{P}_0 for two sets of \bar{k}_r and \bar{k}_s when $\bar{L}_1=0.8$

The point is shown in Fig.1 and its distance to the tip of the beam is \bar{x}_s . In this study the Newmark method (Craig and Kurdila, 2006) is used to solve Eq.(8) for finding the displacement of any point especially the mentioned point. One particular case is selected for this analysis, which is $\bar{L}_1=0.6$, $\bar{k}_r=5000$ and $\bar{k}_s=5000$. The first instability for this case is flutter and happens when $\bar{P}_{ocr}=109.7$. It is also assumed that $\bar{x}_s=0.2 \times \bar{L}_1$ and $\bar{x}_{F_0}=1-\bar{L}_1$.

To start the analysis, it has been assumed that the controller force does not exist ($\bar{F}_0(\bar{t})=0$). One example for a follower force less than critical one, $\bar{P}_0=90$, is analyzed and the displacement and the rate of this point are shown in Fig.13. The figure shows that when the follower force is less than the critical force, the amplitude of the displacement remains constant. Fig.13d shows the trajectory of the

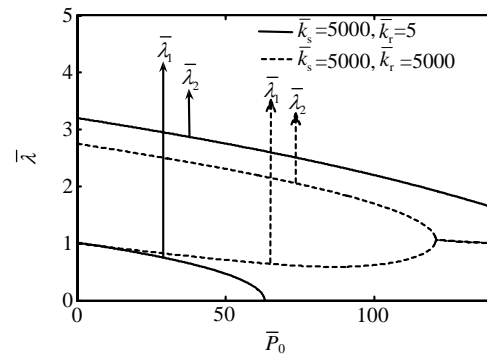


Fig.10 Variations of the first and second non-dimensional natural frequencies vs the non-dimensional follower force \bar{P}_0 for two sets of \bar{k}_r and \bar{k}_s when $\bar{L}_1=0.8$

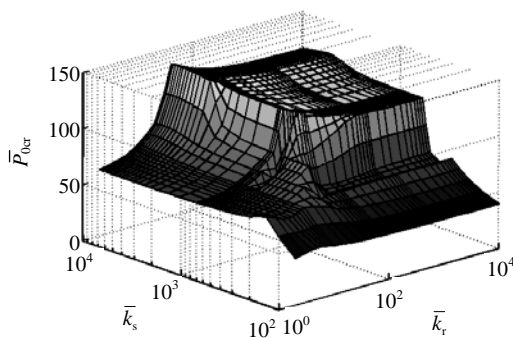


Fig.11 Effects of variation of \bar{k}_r and \bar{k}_s on the non-dimensional critical follower force (\bar{P}_{ocr}) when $\bar{L}_1=0.8$

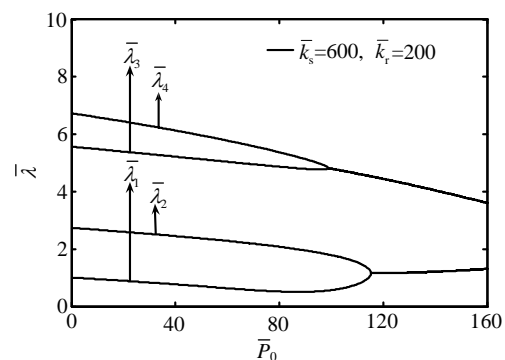


Fig.12 The first instability occurs because of the convergence of the third and the fourth natural frequencies when $\bar{k}_r=200$, $\bar{k}_s=600$ and $\bar{L}_1=0.8$

assumed case. The stability of this system can be concluded using stability in the sense of Lyapunov. Fig.14 presents the displacement and the rate for a point at $\bar{x}_s=0.2 \times \bar{L}_1$ over the time for the same initial condition and for an over-critical force, $\bar{P}_0=128$. The amplitude of the displacement increases periodically. Fig.14d shows the trajectory for this condition and it clearly states that with stability in the sense of Lyapunov, the system is instable.

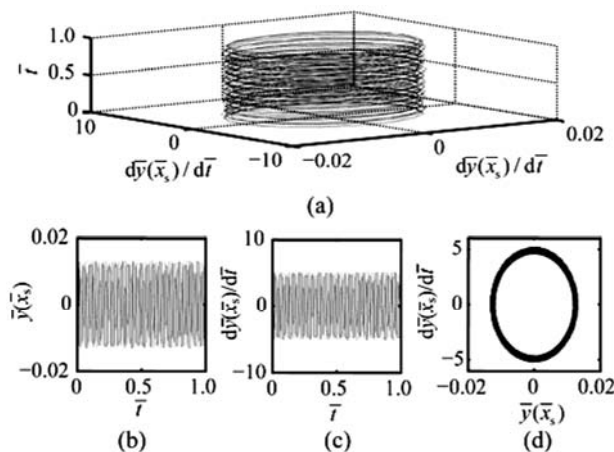


Fig.13 The displacement and the rate of point \bar{x}_s for the assumed initial condition, $\bar{F}_0(\bar{t}) = 0$ and $\bar{P}_0 = 90$

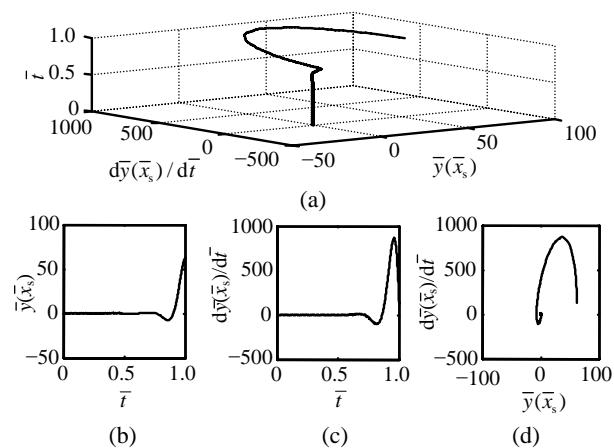


Fig.14 The displacement and the rate of point \bar{x}_s for the assumed initial condition, $\bar{F}_0(\bar{t}) = 0$ and $\bar{P}_0 = 128$

To demonstrate the effects of the transversal force and the follower force ($\bar{F}_0(\bar{t}), \bar{P}_0$) on the amplitude of the displacement at point \bar{x}_s , only one example is used. In this example it has been assumed

that $\bar{x}_s=0.2 \times \bar{L}_1$ and $\bar{x}_{F_0}=1-\bar{L}_1$. Two under-critical follower forces $\bar{P}_0=50$ and 100 are applied (where the critical non-dimensional force is $\bar{P}_0=109.7$). Also two amounts for the transversal force are considered in the example of $\bar{F}_0(\bar{t})=0.01\sin(2\bar{t})$ and $0.02\sin(2\bar{t})$. The amount of transversal force is set to be smaller than that of follower force and the transversal force frequency is also smaller than the natural frequencies of the model.

The effects on the amplitude of the displacement are shown in Fig.15. The amplitude of the displacement is increased when the follower force or the transversal force is increased.

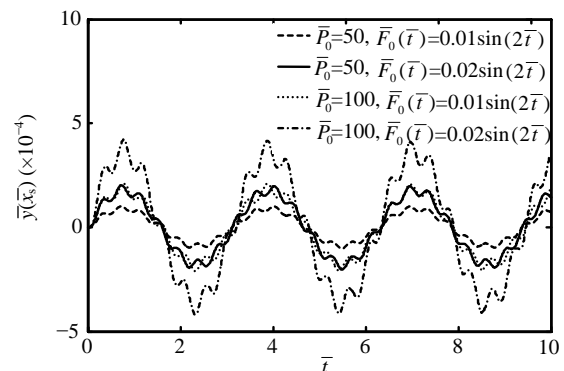


Fig.15 Effects of increasing the follower force and the transversal force on displacement of IMU

CONCLUSION

In this paper the instability and vibrations of a free-free jointed bipartite Bernoulli beam, TSTO LV, under the follower and transversal forces are analyzed. The follower force is the model for the propulsion force and the transversal force is the controller force. Two parts of the beam are jointed by two rotational (\bar{k}_r) and shear springs (\bar{k}_s). The variations of the springs stiffness would change the critical follower force as well as the type of the instability unpredictably. The results show that the dominant instability of the beam is flutter when the joint is located in the top half of the beam. As the joint location gets down to the half, the third natural frequency is also playing an important role in the flutter instability as shown in case $\bar{L}_1=0.4$. When the joint loca-

tion is in the second half, i.e., $\bar{L}_1=0.6$ and $\bar{L}_1=0.8$, both divergence and flutter become the instability modes. In the case $\bar{L}_1=0.6$, flutter occurs due to the convergence of the first and the second natural frequencies only. When the joint location gets closer to the beam end (where the follower force is applied), flutter could also happen due to the convergence of the third and the fourth natural frequencies.

The results offer an approximation method to design the joint location and springs for a free-free jointed bipartite Bernoulli beam under the follower force. For all the under-critical follower forces, the amplitude of any point of the beam especially the IMU location remains constant while it will be unstable when the follower force is equal to or more than the critical one. In the flutter regime, the displacement of any point increases periodically. And in the divergence regime, the displacement instantly increases. By increasing the follower or the transversal force, the amplitude of the IMU location is also increased, which is not desirable for any control system. This study introduces a new concept of parametric study to analyze the effects of the characteristics of a flexible joint of a two-stage aerospace structure that could be considered during its design.

References

- Attard, M.M., Lee, J.S., Kim, M.Y., 2008. Dynamic stability of shear-flexible beck's columns based on Engesser's and Haringx's buckling theories. *Computers and Structures*, **86**(21-22):2042-2055. [doi:10.1016/j.compstruc.2008.04.012]
- Au, F.T.K., Zheng, D.Y., Cheung, Y.K., 1999. Vibration and stability of non-uniform beams with abrupt changes of cross-section by using C1 modified beam vibration functions. *Applied Mathematical Modelling*, **23**(1):19-34. [doi:10.1016/S0307-904X(98)10045-8]
- Beal, T.R., 1965. Dynamic stability of a flexible missile under constant and pulsating thrusts. *AIAA Journal*, **3**(3):486-494. [doi:10.2514/3.2891]
- Bokaian, A., 1988. Natural frequencies of beam under compressive axial loads. *Journal of Sound and Vibration*, **126**(1):49-65. [doi:10.1016/0022-460X(88)90397-5]
- Craig, R.R.Jr., Kurdila, A.J., 2006. Fundamentals of Structural Dynamics. John Wiley & Sons Inc., New Jersey, p.513-527.
- de Rosa, M.A., Auciello, N.M., Lippiello, M., 2008. Dynamic stability analysis and DQM for beams with variable cross-section. *Mechanics Research Communications*, **35**(3):187-192. [doi:10.1016/j.mechrescom.2007.10.010]
- Detinko, F.M., 2003. Lumped damping and stability of Beck column with a tip mass. *International Journal of Solids and Structures*, **40**(17):4479-4486. [doi:10.1016/S0020-7683(03)00298-1]
- Di Egidio, A., Luongo, A., Paolone, A., 2007. Linear and non-linear interactions between static and dynamic bifurcations of damped planar beams. *International Journal of Non-Linear Mechanics*, **42**(1):88-98. [doi:10.1016/j.ijnonlinmec.2006.12.010]
- Djondjorov, P.A., Vassilev, V.M., 2008. On the dynamic stability of a cantilever under tangential follower force according to Timoshenko beam theory. *Journal of Sound and Vibration*, **311**(3-5):1431-1437. [doi:10.1016/j.jsv.2007.10.005]
- Elfelsoufi, Z., Azrar, L., 2006. Integral equation formulation and analysis of the dynamic stability of damped beams subjected to subtangential follower forces. *Journal of Sound and Vibration*, **296**(4-5):690-713. [doi:10.1016/j.jsv.2006.01.019]
- Hassanpour, P.A., Cleghorn, W.L., Mills, J.K., Esmailzadeh, E., 2007. Exact solution of the oscillatory behavior under axial force of a beam with a concentrated mass within its interval. *Journal of Vibration and Control*, **13**(12):1723-1739. [doi:10.1177/1077546307076285]
- Hodges, D.H., Pierce, G.A., 2002. Introduction to Structural Dynamics and Aeroelasticity. The Press Syndicate of the University of Cambridge, Cambridge, p.59-66.
- Joshi, A., 1995. Free vibration characteristics of variable mass rocket having large axial thrust/acceleration. *Journal of Sound and Vibration*, **187**(4):727-736. [doi:10.1006/jsvi.1995.0559]
- Katsikadelis, J.T., Tsiatas, G.C., 2007. Optimum design of structures subjected to follower forces. *International Journal of Mechanical Sciences*, **49**(11):1204-1212. [doi:10.1016/j.ijmecsci.2007.03.011]
- Kim, J.H., Choo, Y.S., 1998. Dynamic stability of a free-free Timoshenko beam subjected to a pulsating follower force. *Journal of Sound and Vibration*, **216**(4):623-636. [doi:10.1006/jsvi.1998.1717]
- Langthjem, M.A., Sugiyama, Y., 1999. Optimum shape design against flutter of a cantilevered column with an end-mass of finite size subjected to a non-conservative load. *Journal of Sound and Vibration*, **226**(1):1-23. [doi:10.1006/jsvi.1999.2211]
- Lee, J.S., Kim, N.I., Kim, M.Y., 2007. Sub-tangentially loaded and damped Beck's columns on two-parameter elastic foundation. *Journal of Sound and Vibration*, **306**(3-5):766-789. [doi:10.1016/j.jsv.2007.06.017]
- Luongo, A., Di Egidio, A., 2006. Divergence, Hopf and double-zero bifurcations of a nonlinear planar beam. *Computers and Structures*, **84**(24-25):1596-1605. [doi:10.1016/j.compstruc.2006.01.004]
- Marzani, A., Tornabene, F., Viola, E., 2008. Nonconservative stability problems via generalized differential quadrature method. *Journal of Sound and Vibration*, **315**(1-2):176-196. [doi:10.1016/j.jsv.2008.01.056]
- Meirovitch, L., 1997. Principles and Techniques of Vibrations. Prentice-Hall International Inc., New Jersey, p.368-371.

- Mladenov, K.A., Sugiyama, Y., 1997. Stability of a jointed free-free beam under end rocket thrust. *Journal of Sound and Vibration*, **199**(1):1-15. [doi:10.1006/jsvi.1996.0625]
- Nihous, G.C., 1997. On the continuity of boundary value problem for vibrating free-free straight beams under axial loads. *Journal of Sound and Vibration*, **200**(1):110-119. [doi:10.1006/jsvi.1996.0642]
- Paolone, A., Vastab, M., Luongoc, A., 2006. Flexural-torsional bifurcations of a cantilever beam under potential and circulatory forces I. Non-linear model and stability analysis. *International Journal of Non-Linear Mechanics*, **41**(4):586-594. [doi:10.1016/j.ijnonlinmec.2006.02.006]
- Park, Y.P., 1987. Dynamic stability of a free Timoshenko beam under a controlled follower force. *Journal of Sound and Vibration*, **113**(3):407-415. [doi:10.1016/S0022-460X(87)80129-3]
- Park, Y.P., Mote, C.D.Jr., 1985. The maximum controlled follower force on a free-free beam carrying a concentrated mass. *Journal of Sound and Vibration*, **98**(2):247-256. [doi:10.1016/0022-460X(85)90388-8]
- Pourtakdoust, S.H., Assadian, N., 2004. Investigation of thrust effect on the vibrational characteristics of flexible guided missiles. *Journal of Sound and Vibration*, **272**(1-2):287-299. [doi:10.1016/S0022-460X(03)00779-X]
- Ryu, S.U., Sugiyama, Y., 2003. Computational dynamics approach to the effect of damping on stability of a cantilevered column subjected to a follower force. *Computers and Structures*, **81**(4):265-271. [doi:10.1016/S0045-7949(02)00436-4]
- Sato, K., 1991. On the governing equation for vibrating and stability of a Timoshenko beam: Hamilton's Principle. *Journal of Sound and Vibration*, **145**(2):338-340. [doi:10.1016/0022-460X(91)90597-D]
- Shvartsman, B.S., 2007. Large deflections of a cantilever beam subjected to a follower force. *Journal of Sound and Vibration*, **304**(3-5):969-973. [doi:10.1016/j.jsv.2007.03.010]
- Sugiyama, Y., Langthjem, M.A., 2007. Physical mechanism of the destabilizing effect of damping in continuous non-conservative dissipative systems. *International Journal of Non-Linear Mechanics*, **42**(1):132-145. [doi:10.1016/j.ijnonlinmec.2006.11.011]
- Thana, H.K., Ameen, M., 2007. Finite element analysis of dynamic stability of skeletal structures under periodic loading. *Journal of Zhejiang University SCIENCE A*, **8**(2):245-256. [doi:10.1631/jzus.2007.A0245]
- Tomski, L., Szmidla, J., Uzny, S., 2007. The local and global instability and vibration of systems subjected to non-conservative loading. *Thin-walled Structures*, **45**(10-11):945-949. [doi:10.1016/j.tws.2007.08.019]
- Wang, Q., 2004. A comprehensive stability analysis of a cracked beam subjected to follower compression. *International Journal of Solids and Structures*, **41**(18-19):4875-4888. [doi:10.1016/j.ijsolstr.2004.04.037]
- Wu, J.J., 1975. On the stability of a free-free beam under axial thrust subjected to directional control. *Journal of Sound and Vibration*, **43**(1):45-52. [doi:10.1016/0022-460X(75)90203-5]
- Young, T.H., Juan, C.S., 2003. Dynamic stability and response of fluttered beams subjected to random follower forces. *International Journal of Non-Linear Mechanics*, **38**(6):889-901. [doi:10.1016/S0020-7462(02)00035-5]